Competing Interactions in Arrested States of Colloidal Clays

B. Ruzicka,[1] L. Zulian,[2] E. Zaccarelli,[1] R. Angelini,[1] M. Sztucki,[3] A. Moussaïd,[3] and G. Ruocco[1]
[1]*SOFT INFM-CNR and Dipartimento di Fisica, Sapienza Università di Roma, I-00185, Italy*
[2]*ISMAC-CNR via Bassini 15, 20133 Milano, Italy*
[3]*European Synchrotron Radiation Facility. Boîte Postale 220, F-38043 Grenoble Cedex, France*

(Received 14 October 2009; published 24 February 2010)

Using experiments, theory and simulations, we show that the arrested state observed in a colloidal clay at high concentrations is stabilized by screened Coulomb repulsion (Wigner glass). Dilution experiments allow us to distinguish this disconnected state, which melts upon addition of water, from a low-concentration gel state, which does not melt. Theoretical modeling and simulations at high concentrations reproduce the measured small angle x-ray scattering static structure factors and confirm the long-range electrostatic nature of the arrested structure. These findings are attributed to the different time scales controlling the competing attractive and repulsive interactions.

DOI: 10.1103/PhysRevLett.104.085701 PACS numbers: 64.70.pv, 64.70.kj

Dynamical arrest in soft colloidal systems has recently become the subject of intense research activity. The fine-tuning of the control parameters opens the possibility to tailor the macroscopic properties of the resulting nonergodic states. Several mechanisms of dynamical arrest have been identified. Building on knowledge of hard sphere glass [1], it has become recently clear that when both attractive and repulsive terms are present in the interaction potential, a reentrant liquid-glass line, surrounded by two distinct glasses, is found at high concentrations [2]. A rich phenomenology also takes place at low concentrations: here gelation occurs, which may result from different routes [3]. Interesting scenarios arise when, in addition to a short-ranged attraction, particles have a residual electrostatic charge which builds up a long-range repulsion in the effective potential. In this case, particles can form equilibrium clusters [4], which provide the building blocks of arrest [5]. Recent works have shown that both Wigner glasses [6], intended as arrested states formed by disconnected particles or clusters and stabilized by the electrostatic repulsion, and equilibrium gels, which occur at larger packing fractions when the clusters branch into a percolating network, can form under these conditions [7,8].

To investigate the formation of multiple arrested states, colloidal clays [9,10] have emerged as suitable candidates. The anisotropy of the particles, combined with the presence of attractive and repulsive terms in the interactions, makes the phase diagram of such colloidal systems very complex. Among these, Laponite suspensions have been widely studied for their appealing industrial applications as well as for their interesting properties [11–18]. In particular, Laponite displays a nontrivial aging dynamics [14] and (at least) two final arrested states, which are obtained by a simple increase of Laponite volume fraction from low ($C_w < 2.0\%$) to high ($C_w \geq 2.0\%$) values, at fixed salt concentration $C_s = 10^{-4}M$ [14,15]. More recently, the static properties of these two states have been investigated in detail [16], showing that they can be differentiated also by the aging properties of the static structure factor $S(Q)$. While the low C_w state has an inhomogeneous character, the high C_w state is homogenous, allowing for the identification of these two arrested states, respectively, as gel and glass.

In this Letter, through the combination of experiments, numerical and theoretical approaches, we demonstrate that the nonergodic state observed in Laponite samples in salt free water at high concentrations ($C_w \geq 2.0\%$) is a Wigner glass. By performing a simple but impressive dilution experiment, we are able to distinguish whether attractive or repulsive interactions are dominant in the formation and stability of the arrested structure for both low- and high-concentration samples. Moreover, we compare $S(Q)$ measured with small angle x-ray scattering (SAXS) with theoretical and numerical calculations in the high-concentration window, providing an estimate for the effective interactions between Laponite platelets. Thereby Laponite not only displays two distinct nonergodic states differing only in colloidal concentration, but also shows a counterintuitive scenario which involves gel-like structures at lower concentrations and a (truly) disconnected glass at larger (but still very low) ones. Hence, the increase of concentration, which normally favors percolation and branching, here has the opposite effect. We attribute this novel behavior to the interplay of different time scales in the involved attractive and repulsive interactions, a feature that may be found in other complex colloidal systems.

To investigate the glassy state formed by Laponite at high clay concentration ($C_w \geq 2.0\%$) [14–16], we use a combination of different approaches. First, we perform a dilution experiment, adding water to the arrested state, to establish the dominant interactions ruling arrest [3]. If this is generated by attraction, the presence of additional water should not affect it, because Laponite bonds (of strong electrostatic nature) can not be broken. On the other hand, if the nonergodic state is stabilized by repulsion, the increase of free volume should allow a rearrangement of the Laponite platelets on average to a larger distance. If such distance is larger than the characteristic repulsive length (namely the electrostatic Debye length) the glass will be destabilized up to melting to a liquid state.

To obtain reliable and reproducible results [19] Laponite RD dispersions are prepared using the same protocol described in [16]. The starting waiting time ($t_w = 0$) is the time at which the suspension is filtered. For the dilution experiment a sample at high clay concentration, $C_w = 3.0\%$, is filtered and sealed in small glass bottles. The photographic sequence of this experiment is shown in Fig. 1. The initially liquid (**L**) [(a) panel] sample ages with time ≈50 h [14] until reaching a final arrested state, as it can be seen in panel (b) where the sample shows its solidlike nature ($\mathbf{G_2}$). At this point a solution of colored water of the same volume as that of the Laponite solution is added to the arrested (colorless) sample to better distinguish [(c) panel] the arrested sample ($\mathbf{G_2}$) from the liquid solution (**L**). After the addition of water, the arrested sample starts to fluidize at the interface with the liquid solution [(d) panel—$t_w = 70$ h]. This process evolves with time until, after 120 h, the whole sample is back into a liquid state [(e) panel]. This result strongly speaks in favor of the repulsive nature of the $C_w = 3.0\%$ arrested state. The experiment is repeated in absence of colorant and shows that the addition of the dye does not affect the results.

We now turn to elucidate the effective interactions between Laponite platelets, by comparing the evolution of the experimental static structure factor $S^M(Q)$, obtained from SAXS measurements performed at the High Brilliance beam line (ID2) [20] at the European Synchrotron Radiation Facility (ESRF) in Grenoble, France, as described in [16], with that predicted theoretically $S^{\rm th}(Q)$, assuming several effective interaction potentials [21].

In Fig. 2 the comparison between $S^M(Q)$ (symbols) and optimal $S^{\rm th}(Q)$ (lines), for fixed $t_w \simeq 50$ h in the concentration window $2.0\% \leq C_w \leq 3.0\%$, is shown. As it is evident from Fig. 2, as concentration is decreased from $C_w = 3.0\%$ to $C_w = 2.0\%$ the low Q signal is slightly increased and the main peak is slightly shifted towards lower Q values. The position of the main peak is around $Q \sim 0.17$ nm^{-1}, corresponding to a length ≈37 nm, a value clearly larger than the platelet diameter $d = 25$ nm, pointing to a nonconnected final structure. Moreover, no evidence of a peak at contact distance is found.

The theoretical $S^{\rm th}(Q)$ is calculated by solving numerically the Ornstein-Zernike equation with an appropriate closure relation [22] or by direct simulation of the effective potential, without a significant change in the description of the experimental data. For simplicity, we report Percus-Yevick results in the following. In this simplified treatment, we consider only the centers of mass of the scattering objects, supposedly single platelets, and treat them as (spherical) points, following previous work on different systems [7]. The main fit parameters involved in the description of the experimental data are the number density ρ of the scattering objects and the number of counter-ions $N_{\rm ci}$ that dissociate (on average) from each platelet when dissolved in water. Our study indicates that ρ cannot be the same as the number density of Laponite discs obtained from the nominal weight concentration $\rho_L = 2.4 \times 10^{22}/m^3$. Indeed, no simple interaction potential is able to reproduce the position of the main peak using ρ_L. Hence ρ must be smaller, due to the fact that platelets may be found within a distribution of clusters [23]. We find that the data can be fully described, in terms of peak position, peak height and compressibility, by a Yukawa potential, which accounts in an average way [7] for the screened electrostatic repulsion between Laponite platelets or clusters, in agreement with more sophisticated theoretical approaches [17]. We use a potential of the form $V_{\rm eff} = A\xi e^{-r/\xi}/r$, where ξ is the Debye screening length and A provides a measure of the repulsion strength. The number density is fixed to $\rho \simeq 0.38\rho_L$, a relationship which is found to hold in the whole investigated concentration window. This suggests that Laponite may be dispersed in a distribution of very small aggregates, possibly due to particles that are not completely delaminated, compatibly with an AFM study performed under very dilute conditions [23]. The number of counterions in solution is optimized to $N_{\rm ci} = 60$, a value well below the bare charge of a single platelet ($700e$), in good agreement both with previous simulations [17] and with conductivity measurements [15]. With this choice of parameters, the changes in nominal concentration and its associated screening length ξ, are able to reproduce $S^M(Q)$ in the full investigated window, as seen in Fig. 2. The

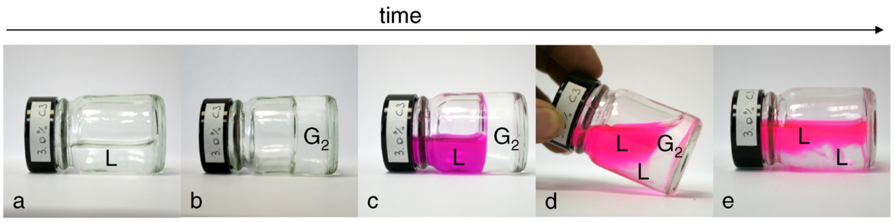

FIG. 1 (color online). Photographic time sequence of the dilution experiment for a high-concentration sample ($C_w = 3.0\%$). The initially liquid (**L**) sample (a) ages with time reaching, after 50 h, a final arrested glassy state ($\mathbf{G_2}$) (b). At this time a colored solution is prepared in a liquid (**L**) state with Rhodamine B at a concentration $10^{-3}M$ with the same volume as the sample. This is added to the arrested sample (c) which starts to fluidize at the interface (d)- 70 h. Finally, the whole sample is liquid again (e)—120 h.

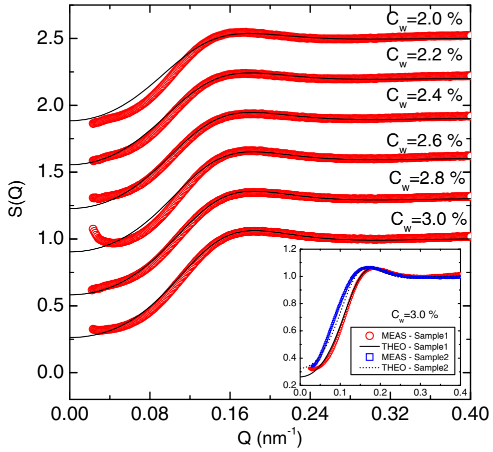

FIG. 2 (color online). Comparison between measured $S^M(Q)$ (symbols) and theoretical $S^{\text{th}}(Q)$ (lines) for several high-concentration samples at $t_w \simeq 50$ h. For clarity, curves have been shifted along the vertical axis progressively by 0.3. Inset: $S^M(Q)$ (symbols) and $S^{\text{th}}(Q)$ (lines) for two different samples with $C_w = 3.0\%$.

repulsion strength $A\xi/k_BT$ is found to increase in the studied range of concentration by a factor of ≈ 2, compatibly with the behavior of other charged systems [24].

While the Yukawa potential correctly reproduces the experimental data, other possible candidates do not. The simple hard sphere model does not capture the softness of the interactions, failing to reproduce the low-Q regime also after one adjusts ρ. On the other hand, the addition of a short-range attraction to the electrostatic repulsion (i) is not sufficient to explain the low Q position of the main peak, and (ii) tends to induce an enhanced structuring at nearest-neighbor length. Hence, the combination of the dilution experiment with the theoretical analysis allows us to identify the observed arrested state as a Wigner glass stabilized by the residual electrostatic repulsion.

One further comment concerns the robustness of our findings when measuring $S^M(Q)$ on different samples, for example taken from different Laponite batches. We find that different samples can be fitted equally well with the effective Yukawa potential slightly adjusting the fit parameters, as shown in the inset of Fig. 2 for two different samples with $C_w = 3.0\%$ prepared from different batches and measured in different runs. For the second batch, which has a higher polydispersity, we find $N_{\text{ci}} = 90$ and $\rho = 0.26\rho_L$.

The theoretical approach we have adopted so far treats only the correlations between the centers-of-mass of the scattering objects. Although such an approach was proven to be a good (although crude) approximation to describe the static correlations between equilibrium clusters of non-spherical shape [7], it is crucial to show that this treatment is valid also when we take into account explicitly the actual disc shape of clay particles. To this aim, we have performed Monte Carlo simulations of 200 discs at the same ρ as that extracted from the fits. We use the interaction model introduced in [25] where the total negative charge is uniformly distributed over the surface area, while rim charges are neglected. Each Laponite platelet is schematized as a rigid disk, composed by 19 sites disposed on a regular mesh. We simulate several repulsion parameters and find that the numerical $S^n(Q)$ is in good agreement with the experimental and theoretical ones when the total charge is fixed to $70e$ and the screening length is 5 nm. Results are shown in Fig. 3 for two samples with $C_w = 2.4\%$ and $C_w = 3.0\%$, in comparison with $S^{\text{th}}(Q)$ and $S^M(Q)$. The favorable comparison of theory and simulations with experimental measurements provides evidence that our effective approach is useful to describe disc-shaped objects in this regime.

So far we have reported evidence of the existence of a Wigner glass state in Laponite by the combination of experiments, theory and simulation for $2.0\% \leq C_w \leq 3.0\%$. At lower concentrations structural measurements have shown a marked growth of $S(Q)$ at low Q with waiting time, which was attributed to the presence of attractive interactions determining an arrested state of attractive (or gel) nature [16]. Already for the lowest concentration shown here ($C_w = 2.0\%$), the agreement between $S^M(Q)$ and $S^{\text{th}}(Q)$ is less good in the low Q range, as visible in Fig. 2. This might be an indication of the increasing role of attractive interactions upon lowering concentration. Hence, we perform the dilution experiment also for a low-concentration sample expecting a different result with respect to the high-concentration one.

In Fig. 4 the dilution experiment is illustrated for a low ($C_w = 1.5\%$) and a high ($C_w = 3.0\%$) concentration sample. The samples are left to age up to the final corresponding arrested states, respectively, of gel ($\mathbf{G_1}$) and glass ($\mathbf{G_2}$) nature for low and high concentrations [16]. While the sample at $C_w = 3.0\%$ arrests within 50 h, the one for $C_w = 1.5\%$ takes several weeks [14,15]. After arrest takes place deionized water ($\mathbf{L}$) is added and panels (a) and (d) show

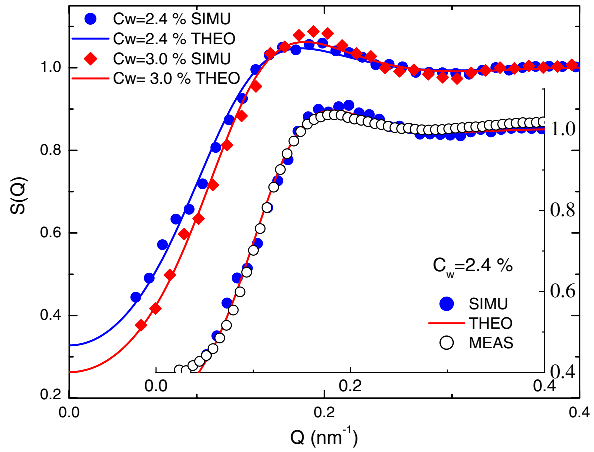

FIG. 3 (color online). Comparison between simulated (symbols) and theoretical (lines) S(Q) for $C_w = 2.4\%$ and 3.0% Laponite samples. Inset: Simulated (closed symbols), theoretical (lines), and measured (open circles) $S(Q)$ for $C_w = 2.4\%$.

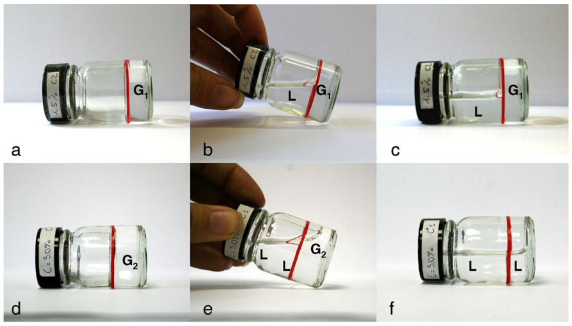

FIG. 4 (color online). Starting (a)–(d), intermediate (b)–(e), and final (c)–(f) states of arrested samples at low $C_w = 1.5\%$ and high $C_w = 3.0\%$ concentrations: while the initial gel state $\mathbf{G_1}$ is not macroscopically affected by the addition of water (c), the glassy state $\mathbf{G_2}$ fluidizes (f).

the identical situation for the two cases. However, the evolution of the two samples soon becomes dramatically different. The arrested state of the high-concentration sample ($\mathbf{G_2}$) starts to fluidify [(e) panel] up to reach a final liquid state [(f) panel]. On the contrary, the low-concentration sample does not show any macroscopic changes of its solid like state, even after waiting additional weeks, i.e., the same time scale of the arrest process. In this case the presence of available free volume does not melt the gel-arrested state [(b) and (c) panels], due to the fact that water cannot break clay bonds. The different behavior between the two samples [(c) and (f) panels] upon dilution confirms the different nature of the two arrested states: a Wigner glass ($\mathbf{G_2}$) and a gel ($\mathbf{G_1}$), dominated, respectively, by repulsive and attractive interactions at high and low concentrations.

The striking result of a low-concentration gel network and of a high-concentration disconnected Wigner glass is at odds with previous studies of simpler systems [7,8,26]. We attribute this unexpected scenario to the separate time scales controlling the interactions and the two arrest processes [14]. While repulsion is felt almost immediately after samples are prepared, attraction, due to its anisotropic nature and to the presence of an effective repulsive barrier, develops on a much longer time scale as in reaction-limited aggregation. Longtime attraction may also affect the repulsive Wigner glass, through the formation of subsequent additional bonds. Indeed, rheological measurements for rejuvenated samples show a dependence on the idle time waited after the glass is formed [27]. To elucidate this point we have performed an additional dilution experiment on the high-concentration sample waiting one week after dynamical arrest takes place. In this case the system does not melt, probably due to intervening long-time attraction which strengthens the glass. However, the unmelted final state is different from the low concentration one: while the latter remains unchanged and water does not penetrate into it, the former seems to slowly absorb water in the bulk. SAXS measurements show that $S(Q)$ does not change significantly in this time window demonstrating that the disconnected structure of the repulsive glass is preserved despite the intervening attraction, and hence the resulting state cannot be considered an attractive glass.

In conclusion, through the combination of dilution and SAXS experiments, theory and simulations, we have shown the presence of a disconnected Wigner glass state in a charged colloidal clay. This arises at a larger concentration with respect to the one where a gel network is found, thanks to the different time scales controlling the repulsive (short-time) and attractive (long-time) interactions. We expect these findings to be relevant to other complex systems with competing interactions.

We thank F. Sciortino for discussions and ESRF for beam time. E. Z. acknowledges SoftComp NMP3-CT-2004-502235 and ERC-226207-PATCHYCOLLOIDS.

[1] P. N. Pusey and W. van Megen, Nature (London) **320**, 340 (1986).
[2] F. Sciortino, Nature Mater. **1**, 145 (2002).
[3] E. Zaccarelli, J. Phys. Condens. Matter **19**, 323101 (2007).
[4] J. Groenewold and W. K. Kegel, J. Phys. Chem. B **105**, 11 702 (2001).
[5] F. Sciortino *et al.*, Phys. Rev. Lett. **93**, 055701 (2004).
[6] H. M. Lindsay and P. M. Chaikin, J. Chem. Phys. **76**, 3774 (1982).
[7] J. C. F. Toledano, F. Sciortino, and E. Zaccarelli, Soft Matter **5**, 2390 (2009).
[8] C. L. Klix, P. Royall, and H. Tanaka, arXiv:1002.1502v1.
[9] A. Shalkevich *et al.*, Langmuir **23**, 3570 (2007).
[10] M. C. D. Mourad *et al.*, J. Phys. Chem. B **113**, 11 604 (2009).
[11] A. Mourchid *et al.*, Langmuir **14**, 4718 (1998).
[12] D. Bonn *et al.*, Europhys. Lett. **45**, 52 (1999).
[13] P. Mongondry, J. F. Tassin, and T. Nicolai, J. Colloid Interface Sci. **283**, 397 (2005).
[14] B. Ruzicka, L. Zulian, and G. Ruocco, Phys. Rev. Lett. **93**, 258301 (2004); Langmuir **22**, 1106 (2006).
[15] S. Jabbari-Farouji *et al.*, Phys. Rev. E **78**, 061405 (2008).
[16] B. Ruzicka *et al.*, Phys. Rev. E **77**, 020402(R) (2008).
[17] E. Trizac *et al.*, J. Phys. Condens. Matter **14**, 9339 (2002).
[18] S. Mossa, C. De Michele, and F. Sciortino, J. Chem. Phys. **126**, 014905 (2007).
[19] H. Z. Cummins, J. Non-Cryst. Solids **353**, 3891 (2007).
[20] T. Narayanan *et al.*, Phys. Rev. Lett. **96**, 258301 (2006).
[21] C. N. Likos, Phys. Rep. **348**, 267 (2001).
[22] J.-P. Hansen and I. R. MacDonald, *Theory of Simple Liquids* (Academic, London, 2006), 3rd ed.
[23] E. Balnois, S. Durand-Vidal, and P. Levitz, Langmuir **19**, 6633 (2003).
[24] F. Cardinaux *et al.*, Europhys. Lett. **77**, 48 004 (2007).
[25] S. Kutter *et al.*, J. Chem. Phys. **112**, 311 (2000).
[26] A. I. Campbell *et al.*, Phys. Rev. Lett. **94**, 208301 (2005).
[27] A. Shanin and Y. Joshi, arXiv:1001.4676.